COD: A Cooperative Cell Outage Detection Architecture for Self-Organizing Femtocell Networks

Wei Wang, *Student Member, IEEE*, Qing Liao, *Student Member, IEEE*, and Qian Zhang, *Fellow, IEEE*

***Abstract*—The vision of Self-Organizing Networks (SON) has been drawing considerable attention as a major axis for the development of future networks. As an essential functionality in SON, cell outage detection is developed to autonomously detect macrocells or femtocells that are inoperative and unable to provide service. Previous cell outage detection approaches have mainly focused on macrocells while the outage issue in the emerging femtocell networks is less discussed. However, due to the two-tier macro-femto network architecture and the small coverage nature of femtocells, it is challenging to enable outage detection functionality in femtocell networks. Based on the observation that spatial correlations among users can be extracted to cope with these challenges, this paper proposes a Cooperative femtocell Outage Detection (COD) architecture which consists of a trigger stage and a detection stage. In the trigger stage, we design a trigger mechanism that leverages correlation information extracted through collaborative filtering to efficiently trigger the detection procedure without inter-cell communications. In the detection stage, to improve detection accuracy, we introduce a sequential cooperative detection rule to process spatially and temporally correlated user statistics. Numerical studies for a variety of femtocell deployments and configurations demonstrate that COD outperforms the existing scheme in both communication overhead and detection accuracy.**

***Index Terms*—Femtocell, self-organizing networks, cell outage detection.**

I. Introduction

SELF-ORGANIZING NETWORKS (SON) have recently been recognized as an attractive paradigm for the next-generation cellular systems by standardization bodies [1], which enables autonomic features in networks, including self-configuration, self-optimization and self-healing. In the self-healing mechanism, cell outage detection is considered to be one of the fundamental functionalities, which aims to autonomously detect cells in an *outage* state, i.e., cells that are inoperable and cannot provide any service due to hardware failures, software failures or even misconfigurations [1]. Cell outage often results in decreased capacity and coverage gap. Such degraded performance leads to high user churn rate and operational expenditures. However, detecting outaged cells is non-trivial. The outaged cells cannot be detected by Operations Support System (OSS) when the detection systems of the outaged cells malfunction [2]. In addition, it is difficult for the cellular system management functions to detect outaged cells directly when the outage is caused by misconfigurations. Identifying these outaged cells usually requires unplanned site visits and usually takes hours or even days. To reduce manual costs and detection delay, the cell outage detection function is proposed in [1] to automatically identify the outaged cells by users' performance statistics analysis.

Most, if not all, previous cell outage detection approaches have focused on macrocells [3], [4]. However, traditional macrocell networks are likely to be supplemented with smaller femtocells deployed within homes and enterprise environments in the next-generation cellular networks [5], where outage occurs more frequently because of inappropriate indoor human interactions and unplanned deployments of large numbers of femto access points (FAPs). Unfortunately, when applied to femtocell networks, existing macrocell outage detection works fall short due to the distinct features of femtocell networks.

- **Dense deployments**. Since there are normally tens or hundreds of femtocells deployed within a macrocell, the number of femtocells is much larger compared with macrocells. The centralized statistics analysis adopted by macrocell outage detection approaches [3], [4] will involve high communication overhead if applied directly in femtocell networks, which will degrade the femtocell service.
- **Vertical handover**. Femtocell users can vertically handover between femtocell and macrocell. However, this vertical handover issue is not considered in the existing macrocell outage detection approaches [3], [4]. In the two-tier femto-macro cellular networks, when a femtocell outage occurs, its users may handover to macrocell and be unaware of the outage. This can be misleading in the user statistics analysis.
- **Sparse user statistics**. Unlike macrocell with large coverage, small scale indoor femtocell usually only supports a few active users (typically 1 to 4 active mobile phones in a residential setting). Macrocell approaches [3], [4], which are based on user statistics within one cell, however, fall inaccurate due to the sparsity of user statistics with high uncertainty caused by severe indoor shadow fading. In the worst case, femtocell with small coverage may have no active users in certain time slots, leading to the failure of these algorithms.

To overcome the aforementioned challenges in femtocell networks, we propose an efficient detection architecture, referred

Manuscript received September 11, 2013; revised February 26, 2014 and May 18, 2014; accepted September 16, 2014. Date of publication September 30, 2014; date of current version November 7, 2014. This work was support in part by grants from 973 project 2013CB329006, China NSFC under Grant 61173156, RGC under Contracts CERG 622410, 622613, HKUST6/CRF/12R, and M-HKUST609/13, as well as the grant from Huawei-HKUST joint lab. The associate editor coordinating the review of this paper and approving it for publication was A. Kwasinski.

The authors are with the Department of Computer Science and Engineering, Hong Kong University of Science and Technology, Kowloon, Hong Kong (e-mail: gswwang@cse.ust.hk; qnature@cse.ust.hk; qianzh@cse.ust.hk).

Color versions of one or more of the figures in this paper are available online at http://ieeexplore.ieee.org.

Digital Object Identifier 10.1109/TWC.2014.2360865

to as *COD* (**C**ooperative femtocell **O**utage **D**etection), which consists of an intra-cell trigger stage and an inter-cell detection stage. The core idea of this architecture includes the following considerations: 1) To reduce communication overhead, the trigger procedure runs on each FAP in a distributed manner without any inter-cell communications. We design a low cost mechanism to trigger the detection for possible outage femtocell via long term passive monitoring of users' *Reference Signal Received Power* (RSRP) statistics. The RSRP statistics are user's basic physical layer measurements on the linear average of the downlink reference signals across the channel bandwidth. 2) The trigger decisions are based on spatial correlations among users' RSRP statistics, rather than disconnected devices [6], [7] or neighbor list [3] as in traditional approaches. The RSRP statistics correlations are leveraged to distinguish the vertical handover case and the outage case. 3) To cope with the data sparsity issue, a detection rule enables neighboring femtocells to cooperatively detect outaged femtocells over a certain period of time, so as to expand the statistics over the space domain and the time domain to obtain enough information. A data fusion rule is used to process the statistics to make a final decision.

To the best of our knowledge, this paper is the first work to explore the outage detection problem in the context of femtocell networks. The main contributions of this work can be summarized as follows. First, this paper proposes a correlation based outage detection architecture for the two-tier femtocell networks. Second, a distributed trigger mechanism with provable error bound and convergence guarantee is designed to reduce the communication overhead and to address the vertical handover issue. Third, a cooperative detection rule is proposed to cope with the data sparsity issue by extracting both the spatial and temporal correlations of RSRP statistics over multiple femtocells. Finally, the evaluation results show that the proposed approach outperforms the conventional method in terms of communication cost as well as detection accuracy.

The rest of the paper is organized as follows. Related works are reviewed in Section II. Section III describes the system model. Section IV illustrates the rationale of the proposed COD architecture. Section V introduces the trigger mechanism in COD, and analyzes its convergence property and error bound. Section VI formulates the cooperative outage detection problem in COD as a sequential hypothesis testing problem and derives analytical results. Numerical results are presented in Section VII. Finally, Section VIII concludes the paper.

II. Related Work

SON functions are defined in 3GPP standards [1] to reduce capital and operational expenses by bringing self-configuration, self-optimization, and self-healing abilities to cellular systems [8]. Recently, self-healing issue in cellular networks has also been studied in the research community [9]. Most of these studies have devoted to cell outage compensation [9], which aims at mitigating the degradation of coverage, capacity and service quality caused by cell outage. In this paper, we have focused on the cell outage detection part of self-healing function. Existing cell outage detection schemes have focused on macrocell. In [3], user's neighbor cell list reports are leveraged to construct a visibility graph, whose topology changes are used to detect outaged macrocells. However, these cell outage detection studies do not consider the distinct features of femtocell networks, and thus cannot be directly applied to femtocell outage detection. Mobility robustness optimization (MRO) [10] is a solution for automatic detection and correction of errors in the mobility configuration, while this paper focuses on the outage that total radio services fail. Minimization of driving test (MDT) technique [11] detects outage by comparing the current measurements with pre-stored measurements that model the normal case. The MDT technique is similar to the benchmark data used in this paper, while the difference is that we extract the spatial correlations based on collaborative filtering to cope with the unique challenges in femtocell networks.

Troubleshooting has been studied in previous works [4], [12]. Khanafer *et al.* [4] propose a framework to process historical user statistics via offline Bayesian analysis to diagnose the root causes for the cell outage. Based on a similar but enhanced offline analysis model, Wang *et al.* [12] further study the outage troubleshooting problem in the context of femtocell networks. These works focus on offline analysis of the root causes after an outage has been detected, while we emphasize the online detection of the outaged cell.

III. System Model

Network Model: We consider a typical two-tier femtocell network architecture where a set of femtocells $\mathcal{F} = \{1, \ldots, F\}$ are overlaid on a macrocell. Femtocell f operates under the FAP f. A femtocell experiences outage with certain probability in the process of operation. The outaged FAP cannot transmit or receive any signal. FAPs transmit reference signals periodically in the downlink. The reference signals, which facilitate user's channel measurements (e.g., the RSRP measurement), are sent back to the FAPs as feedback messages.

User Model: The locations of the users are unknown. The users transmit or receive data from their associated FAPs, and periodically report the RSRP statistics of all neighboring cells to their associated FAPs, providing guidance in handover and cell reselection decisions. We assume that the users in an area A follow a Poisson point process with density ρ, i.e., $n_A \sim Poi(n; \rho|A|)$, where n_A is the number of users within the area A.

Channel Model: The channel gains of a user u to an FAP f are determined based on the model described in [13]:

$$h = \left(\frac{d_o}{d_{u,f}}\right)^a e^{X_{u,f}} e^{Y_{u,f}}, \tag{1}$$

where d_o is the reference distance (e.g., 1 m), $d_{u,f}$ the distance between the FAP f to the user u, and a the path loss exponent. $e^{X_{u,f}}$ and $e^{Y_{u,f}}$ are shadow fading factor and multi-path fading factor, respectively. The shadow fading follows a Gaussian distribution described by $X_{u,f} \sim \mathcal{N}(0, \sigma), \forall u, f$. The multi-path fading is modeled by Rayleigh fading with zero mean, and thus $\mathbb{E}[e^Y_{u,f}] = 0$.

Shadow fading effects are assumed to be independent over time. With this assumption, the RSRP statistics of a user are

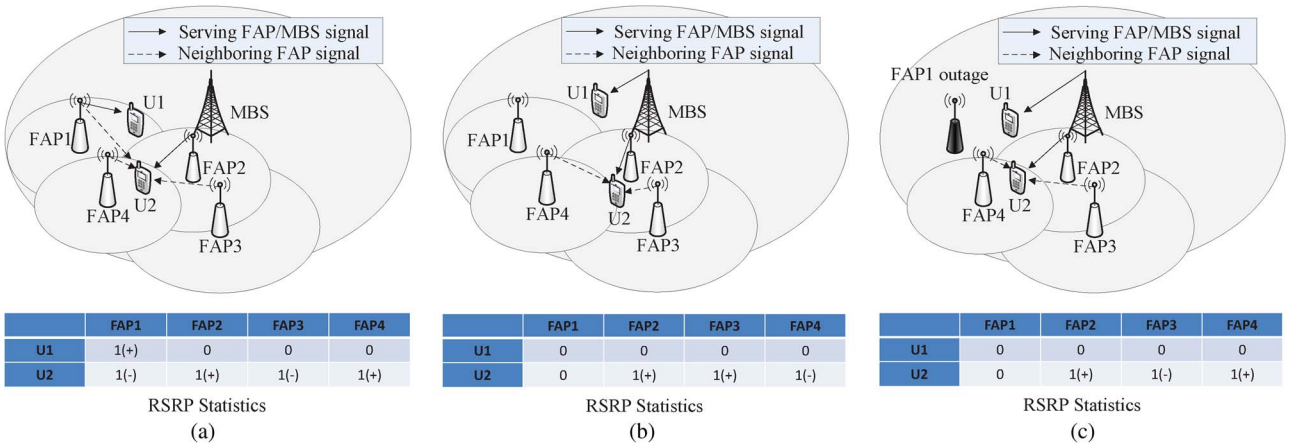

	FAP1	FAP2	FAP3	FAP4
U1	1(+)	0	0	0
U2	1(-)	1(+)	1(-)	1(+)

RSRP Statistics
(a)

	FAP1	FAP2	FAP3	FAP4
U1	0	0	0	0
U2	0	1(+)	1(+)	1(-)

RSRP Statistics
(b)

	FAP1	FAP2	FAP3	FAP4
U1	0	0	0	0
U2	0	1(+)	1(-)	1(+)

RSRP Statistics
(c)

Fig. 1. Cases in femtocell outage detection. (a) Normal case. (b) Vertical handover case. (c) Outage case.

independent random variables. Note that all RSRP statistics of a user can be characterized by (1). As such, the RSRP statistics at a certain user u are independent and identically distributed (i.i.d.), and thus can be approximated as a Gaussian distribution using the *Central Limit Theorem* (CLT). Then, the distribution can be given as [14]:

$$r_u \sim \begin{cases} \mathcal{N}\left(N_o, \frac{{N_o}^2}{M}\right) & \mathcal{H}_0 \\ \mathcal{N}\left(P_u + N_o, \frac{(P_u+N_o)^2}{M}\right) & \mathcal{H}_1 \end{cases} \quad (2)$$

where r_u is user u's RSRP statistics, P_u the received signal strength at user u, N_o the noise power, and M the number of signal samples, e.g., 5×10^3/ms for 5 MHz band. $\mathcal{H}_0$ stands for the outage case and $\mathcal{H}_1$ for the normal case.

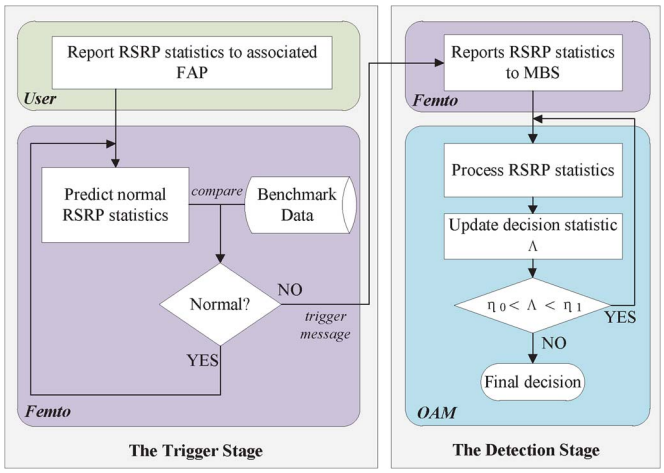

Fig. 2. Architecture overview.

IV. Rationale of the COD Architecture

A. Observation

To design a femtocell outage detection architecture, we first investigate the spatio-temporal correlations in RSRP statistics. In Fig. 1, U2 keeps moving in all the three cases, while U1 remains in the same location in the normal case and the outage case but moves away from FAP1 in the vertical handover case. The tables in Fig. 1 show the corresponding RSRP statistics, which are classified into three levels: $1(+)$ for strong received signal from a certain FAP, $1(-)$ for weak received signals, and 0 for no received signal. Comparing Fig. 1(a) and (c), U2's RSRP statistics from FAP2-FAP4 are the same while the RSRP statistics from FAP1 are different. A previous study [15] shows that users in close proximity have similar signal statistics, and the estimation of location similarity is more accurate when there are more FAPs nearby. Therefore, we can infer that the locations of U2 in Fig. 1(a) and (c) are probably close, and thus the RSRP from FAP1 should be similar in the two figures if FAP1 is normal in Fig. 1(c). Thus, the difference between RSRP statistics from FAP1 in the two figures indicates that FAP1 may be experiencing outage in Fig. 1(c). On the other hand, comparing Fig. 1(a) and (b), the locations of U2 are considered to be quite different since the U2's RSRP statistics from FAP2-FAP4 in both cases have weak correlations. Therefore, even though the RSRP statistics from FAP1 are very different in the two cases, we cannot infer whether FAP1 is experiencing outage or not. Based on the above analysis, we observe that the UE vicinity relations that lie in the RSRP statistics can be used to enhance outage detection. To achieve this goal, an FAP can check the states of neighboring FAPs by comparing current statistics with historical statistics in normal cases.

Based on this observation, we can tackle the vertical handover issue and enable the distributed trigger mechanism. In the trigger mechanism, each femtocell monitors the state of its neighboring femtocells based on correlations between current RSRP statistics and historical RSRP statistics reported by the users. Moreover, multiple femtocells can cooperatively process RSRP statistics by further exploiting the correlations over a period of time to cope with the user sparsity issue.

B. COD Architecture Overview

Fig. 2 illustrates the COD architecture. Before the trigger stage, each FAP stores a copy of *benchmark data* beforehand, which is collected when all FAPs are normal. Benchmark data contains the RSRP statistics from all neighboring FAPs in the form of a matrix $\mathbf{R}$, where element $R_{u,f}$ in $\mathbf{R}$ is the RSRP of user u from FAP f.

In the trigger stage, each FAP runs the trigger algorithm to monitor the states of neighboring femtocells by checking the

reported RSRP statistics from its associated users. To check whether the RSRP statistics are normal or not, the FAP predicts the expected normal RSRP statistics based on the benchmark data via collaborative filtering. As for an FAP i, if the RSRP statistics from a neighboring FAP f deviate from the predicted normal statistics, then FAP i will send a trigger message to the MBS to trigger the detection stage to further decide whether the FAP f is experiencing outage.

In the detection stage, all the FAPs within the cooperation range report the statistics collected in trigger stage to the MBS periodically until the MBS collects enough information to make a final decision. In each iteration, based on the newly reported RSRP statistics, the MBS processes the statistics via data fusion to update decision statistic, and compares it with pre-computed thresholds (i.e. η_0 and η_1), until it is qualified to make a final decision. The thresholds are computed to guarantee the pre-defined false alarm and misdetection rates. If the decision statistic is below the lower threshold (i.e. η_0), the MBS makes a final decision that FAP f is experiencing outage. If the decision statistic is above the higher threshold (i.e. η_1), the MBS decides that FAP f is normal. Otherwise, the MBS continues to take another round and accumulates more RSRP statistics.

V. Collaborative Filtering-Based Trigger Mechanism

A. Trigger Mechanism

The trigger stage contains two steps, namely, the normal RSRP statistics prediction and the trigger decision, as illustrated in Fig. 2. To predict normal RSRP statistics, we leverage the notion of collaborative filtering to explore the correlations among the femtocell users.

Normal RSRP Statistics Prediction: To make a trigger decision, the expected normal RSRP $r_{u,f}$ of a user u from the target FAP f needs to be estimated. The first step is to leverage collaborative filtering to profile users and FAPs by exploiting correlations among them. *Matrix factorization* (MF), which decomposes a matrix as a product of two low-rank latent matrices, is one of the most popular techniques for collaborative filtering with attractive accuracy and scalability. We exploit the correlations of RSRP statistics via MF as follows.

Suppose that the user u is associated with the FAP b and b needs check whether a neighboring FAP f is normal based on $r_{u,f}$. The RSRP statistics of u from all FAP b's neighboring FAPs are denoted as $\mathbf{r}^u \in \mathbb{R}^{1\times m}$, and the benchmark data matrix stored in FAP b is denoted as $\mathbf{R}^b \in \mathbb{R}^{(n-1)\times m}$. Let $\hat{\mathbf{R}} = \left[\begin{smallmatrix}\mathbf{r}^u \\ \mathbf{R}^b\end{smallmatrix}\right]$. Via MF, the RSRP matrix $\hat{\mathbf{R}}$ is transformed into a low-rank matrix $\mathbf{U} \in \mathbb{R}^{n\times d}$ representing user's latent profile and another low-rank matrix $\mathbf{V} \in \mathbb{R}^{m\times d}$ representing FAP's latent profile, where $d \in \mathbb{N}$ is smaller than m, n. $\mathbf{U}$ and $\mathbf{V}$ are computed as follows.

$$\min_{\mathbf{U},\mathbf{V}} \left\| \left(\hat{\mathbf{R}} - \mathbf{U}\mathbf{V}^\top\right) \odot \mathbf{I} \right\|_F^2, \tag{3}$$

where $\|\cdot\|_F$ is the Frobenius norm, and $\odot$ signifies the element-wise multiplication. $\mathbf{I}$ is the index matrix to indicate the expected normal RSRP $\hat{r}_{u,f} \in \mathbb{R}$ that we want to predict by setting the corresponding element in $\mathbf{I}$, e.g., $I_{1,f}$, as 0 while leaving all other elements in $\mathbf{I}$ as 1. We can eliminate $\mathbf{I}$ by replacing the original value of $r_{u,f}$ with "*Any*", where $x - Any = 0, \forall x \in \mathbb{R}$.

However, (3) does not consider the intrinsic geographical structure of femtocells. To remedy this problem, our observation is that the links between a receiver and nearby transmitters experiences similar multipath environments [16], which implies that the nearby FAPs have similar latent profiles. To exploit the geographical structure of femtocells, we leverage the *graph regularized nonnegative MF* (GNMF) [17]. The basic assumption in GNMF is that data points reside on the surface of a manifold that lies in a low-dimensional space. Specifically, GNMF constructs an adjacent graph $\mathbf{G}$ to represent the local geographical structure of users. In $\mathbf{G}$, each node associates an FAP and an edge is established between two nodes if one node belongs to the k nearest neighbors of another. The node distance is measured by the Euclidean distance between FAPs' latent profiles $\{\mathbf{V}_f : \forall f\}$. Based on $\mathbf{G}$, we can build an adjacent matrix $\mathbf{W}$ as follows

$$w_{ij} = \begin{cases} 1, & f_j \in N_k(f_i) \\ 0, & \text{otherwise} \end{cases} \tag{4}$$

where w_{ij} is an element in $\mathbf{W}$ and $N_k(f_i)$ denotes the k nearest neighbors of the FAP f_i. To preserve the geographical structure of FAPs, the objective is to minimize

$$\sum_{i=1}^{n}\sum_{j=1}^{n} \|\mathbf{V}_i - \mathbf{V}_j\|_2^2 W_{ij} = \mathrm{tr}(\mathbf{V}^\top \mathbf{L}\mathbf{V}) \tag{5}$$

where $\mathbf{L} = \mathbf{D} - \mathbf{W}$ is the Laplacian matrix of $\mathbf{G}$, where $\mathbf{D}$ is a diagonal matrix defined by $D_{jj} = \sum_l w_{jl}$, and $\mathrm{tr}(\cdot)$ signifies the trace operator over a symmetric matrix. Considering (3) and (5) together, we arrive at the objective of GNMF

$$\min_{\mathbf{U},\mathbf{V}} \left\| \left(\hat{\mathbf{R}} - \mathbf{U}\mathbf{V}^\top\right) \right\|_F^2 + \lambda \mathrm{tr}(\mathbf{V}^\top \mathbf{L}\mathbf{V}), \tag{6}$$

where $\lambda > 0$ is a trade-off parameter over the manifold regularization term.

To solve Problem (6) efficiently, we proposed a rank-one residue approximation algorithm. Instead of updating the whole $\mathbf{U}$ and $\mathbf{V}$, we recursively update their columns with the remaining variables fixed. For the kth column of $\mathbf{U}$ and $\mathbf{V}$, the subproblems are

$$\min_{\mathbf{U}_{\cdot k}\geq 0} \left\|\mathbf{E}_k - \mathbf{U}_{\cdot k}\mathbf{V}_{\cdot k}^T\right\|_F^2 \tag{7}$$

and

$$\min_{\mathbf{V}_{\cdot k}\geq 0} \left\|\mathbf{E}_k - \mathbf{U}_{\cdot k}\mathbf{V}_{\cdot k}^\top\right\|_F^2 + \lambda \mathbf{V}_{\cdot k}^\top \mathbf{L}\mathbf{V}_{\cdot k}, \tag{8}$$

where $\mathbf{E}_k$ denotes the residue of $\hat{\mathbf{R}}$ after eliminating the kth column of $\mathbf{U}$ and $\mathbf{V}$, i.e., $\mathbf{E}_k = \hat{\mathbf{R}} - \sum_{l\neq k} \mathbf{U}_{\cdot l}\mathbf{V}_{\cdot l}^T$. $\mathbf{U}_{\cdot k}$ and $\mathbf{V}_{\cdot k}$ denote the kth columns of $\mathbf{U}$ and $\mathbf{V}$, respectively. The subproblem (8) is derived from the following equation: $\mathrm{tr}(\mathbf{V}^\top \mathbf{L}\mathbf{V}) = \sum_{k=1}^{d} \mathbf{V}_{\cdot k}^\top \mathbf{L}\mathbf{V}_{\cdot k}$.

The following lemma shows that these two subproblems can be efficiently solved.

Lemma 1: The subproblems (7) and (8) can be solved by updating the columns of $\mathbf{U}$ and $\mathbf{V}$ according to the following rules:

$$\mathbf{U}_{\cdot k} = \frac{\prod_{+}(\mathbf{E}_k \mathbf{V}_{\cdot k})}{\|\mathbf{V}_{\cdot k}\|_2^2}, \tag{9}$$

$$\mathbf{V}_{\cdot k} = \prod_{+}\left(\left(\|\mathbf{U}_{\cdot k}\|_2^2 I + \lambda \mathbf{L}\right)^{-1} \mathbf{E}_k^{\top} \mathbf{U}_{\cdot k}\right), \tag{10}$$

where $\prod_{+}(\cdot)$ is an element-wise projection that shrinks negative entries to zero.

Based on the above lemma, we show that the update rules always converge to the optimal solution.

Theorem 1: Updating the columns of $\mathbf{U}$ and $\mathbf{V}$ according to (9), (10) converges to the optimal solution of the subproblems (7) and (8).

After solving Problem (6), we use the latent profiles $\mathbf{U}$ and $\mathbf{V}$ to predict the normal RSRP $r_{u,f}$. Note that since $I_{u,f}$ is set to 0, the value of $r_{u,f}$ will not affect the computation of $\mathbf{U}, \mathbf{V}$. Then, the missing element $r_{u,f}$ in $\hat{\mathbf{R}}$ can be predicted by $\mathbf{U}$ and $\mathbf{V}$:

$$\hat{r}_{u,f} = \mathbf{U}_u \mathbf{V}_f^{\top}. \tag{11}$$

Trigger Decision: Based on the predicted normal RSRP $\hat{r}_{u,f}$, the trigger decision is made according to the maximum likelihood rule. In particular, $\hat{r}_{u,f}$ is treated as the mean of the normal hypothesis $\mathcal{H}_1$ as defined in (2), the noise power N_o as the mean of the outage hypothesis $\mathcal{H}_0$, and the actual current RSRP $r_{u,f}$ as the test statistic. If the probability of $r_{u,f}$ under $\mathcal{H}_0$ is larger than the probability of $r_{u,f}$ under $\mathcal{H}_1$, the detection stage is triggered. Otherwise, FAP runs the trigger procedure over again on the newly arrived RSRP statistics.

B. Error Bound Analyses for Normal RSRP Prediction

According to the channel model described by (1), the RSRP statistics are largely affected by shadow fading. We denote the true received signal strength matrix without shadow fading as $\mathbf{P}$, whose corresponding RSRP matrix is $\hat{\mathbf{R}}$. If the unit of signal strength is dBm, we have $\hat{\mathbf{R}} = \mathbf{P} + \mathbf{X}$, where $\mathbf{X}$ is the shadow fading matrix with each element following Gaussian distribution $\mathcal{N}(0, \sigma)$. The approximation error with respect to $\mathbf{P}$ is defined to be $\mathcal{E}(\mathbf{P}, \mathbf{U}\mathbf{V}^{\top}) \triangleq \frac{1}{mn}\sum_{i=1}^{m}\sum_{k=1}^{n}|\mathbf{P}_{i,k} - \mathbf{U}_{i,k}\mathbf{V}_{i,k}|$. Then, we derive the upper bound of $\mathcal{E}(\mathbf{P}, \mathbf{U}\mathbf{V}^{\top})$ through the following theorem.

Theorem 2: For any received signal strength matrix $\mathbf{P}$ and shadow fading matrix $\mathbf{X}$ with each element following Gaussian distribution $\mathcal{N}(0, \sigma)$, with probability of at least $1-\delta$, we have

$$\mathcal{E}(\mathbf{P}, \mathbf{U}\mathbf{V}^{\top}) \leq \sum_{i=1}^{m}\sum_{k=1}^{n}\left(\sqrt{\sum_{l=d+1}^{rank(\hat{\mathbf{R}})} o_l^2} + \sum_{l=1}^{d}|1 - o_l|V_{i,l}U_{k,l}\right) + \varepsilon, \tag{12}$$

where ε satisfies $e^{\frac{-\varepsilon^2}{2\sigma^2}}(1 - Q(\varepsilon)) = \delta\frac{1}{mn}/2$.

VI. Sequential Cooperative Detection via Data-Fusion

A. Sequential Hypothesis Testing

We assume that the detection for FAP f is triggered. The vector of test statistics collected in detection round t is denoted as $\boldsymbol{\theta}_t = [r_{1_t}, \ldots, r_{i_t}, \ldots, r_{n_t}]^T$, where r_{i_t} is the user i's RSRP from f in detection round t. n_t is the number of users within the cooperation range R centered by the location of f. As shown in (2), the RSRP statistics can be approximated as a Gaussian distribution in both normal and outage cases. Thus, our outage detection problem is a binary decision problem for deciding whether hypothesis $\mathcal{H}_0$ or $\mathcal{H}_1$ is true, given the test statistics $\boldsymbol{\theta}$, where $\boldsymbol{\theta} = [{\boldsymbol{\theta}_1}^T, \ldots, {\boldsymbol{\theta}_t}^T, \ldots, {\boldsymbol{\theta}_T}^T]$.

To solve the binary decision problem, the MBS keeps collecting new test statistics from users until the amount of information and the resulting testing performance are satisfied. To achieve this goal, we take Wald's *Sequential Probability Ratio Test* (SPRT) [20] as the data processing rule to decide the stopping time of making a final decision. The main advantage of SPRT is that it requires the minimal number of test statistics to achieve the same error probability, which is attained at the expense of additional computation. In the sequential decision process, the MBS computes the log likelihood ratio and compares it with two thresholds η_0 and η_1. It either settles on one of the two hypothesis, or decides to make another round of statistics collection.

The likelihood ratio in detection round t is defined by:

$$\lambda_t = \ln\frac{p(r_{1_t}, \ldots, r_{n_t}|\mathcal{H}_1)}{p(r_{1_t}, \ldots, r_{n_t}|\mathcal{H}_0)} = \sum_{i_t=1}^{n_t}\ln\frac{p(r_{i_t}|\mathcal{H}_1)}{p(r_{i_t}|\mathcal{H}_0)}, \tag{13}$$

where r_{i_t} is approximated as $r_{i_t} \sim \mathcal{N}(\mu_k, \sigma_k)$ under the hypothesis $\mathcal{H}_k$, according to the CLT. Note that ${\sigma_0}^2 = \frac{N_o^2}{M}$ and ${\sigma_1}^2 = \frac{P_u + N_o^2}{M}$, where P_u and N_o are the average received signal power at users and the noise power. In a very low SNR environment, it is reasonable to approximate $(P_u + N_o)$ as N_o, and hence $\sigma_1 \approx \sigma_0$. Then, (13) can be expressed as:

$$\lambda_t = \frac{(\mu_1 - \mu_0)\sum_{i_t=1}^{n_t} r_{i_t} + \frac{1}{2}n_t({\mu_0}^2 - {\mu_1}^2)}{{\sigma_0}^2}. \tag{14}$$

The next step is to determine the decision statistic Λ_T in detection round T. Λ_T is defined to be the joint likelihood ratio of a sequential test statistics. Regarding that the test statistics are Gaussian and i.i.d., we have

$$\Lambda_T = \frac{(\mu_1 - \mu_0)}{{\sigma_0}^2}\sum_{t=1}^{T}\sum_{i_t=1}^{n_t} r_{i_t} + \frac{Tn_t}{2{\sigma_0}^2}({\mu_0}^2 - {\mu_1}^2). \tag{15}$$

The decision of SPRT in detection round T is based on the following rules [20]:

$$\begin{cases} \Lambda_T \geq \eta_1 & \Rightarrow \text{accept } \mathcal{H}_1 \\ \Lambda_T \leq \eta_0 & \Rightarrow \text{accept } \mathcal{H}_0 \\ \eta_0 < \Lambda_T < \eta_1 & \Rightarrow \text{take another detection round,} \end{cases} \tag{16}$$

where η_1 and η_0 are the detection thresholds, which are determined by the predefined values of desired false alarm rate α and misdetection rate β. However, the outage detection problem is

opposite to the detection problem described in [20] in the sense of misdetection rate and false alarm rate, since $\mathcal{H}_0$ is hypothesis for outage occurrence while $\mathcal{H}_1$ for event occurrence in [20]. Thus, the detection thresholds are given by $\eta_1 = \ln \frac{1-\alpha}{\beta}$ and $\eta_0 = \ln \frac{\alpha}{1-\beta}$, where α and β are the desired false alarm rate and misdetection rate, respectively.

B. Average Detection Delay Analysis

The aim of SPRT is to achieve the desired false alarm and misdetection rates with the minimal number of detection rounds, which stands for detection delay. The expected number of detection rounds is computed according to [20]:

$$\mathbb{E}[\Lambda_T] = \mathbb{E}[T] \times \mathbb{E}[\lambda_t]. \tag{17}$$

First, we derive the expectation of Λ_T in normal cases, namely, under hypothesis $\mathcal{H}_1$. According to (16), $\mathcal{H}_1$ is accepted when Λ_T reaches the threshold η_1, otherwise $\mathcal{H}_2$ is accepted (i.e., false alarm). Thus, Λ_T reaches the threshold η_0 with the probability of false alarm rate α and reaches the threshold η_1 with probability $(1-\alpha)$. Then, we derive the expectation of Λ_T under $\mathcal{H}_1$:

$$\mathbb{E}[\Lambda_T|\mathcal{H}_1] = (1-\alpha)\ln\frac{1-\alpha}{\beta} + \alpha \ln \frac{\alpha}{1-\beta}. \tag{18}$$

Similarly, we derive the expectation of Λ_T under $\mathcal{H}_0$:

$$\mathbb{E}[\Lambda_T|\mathcal{H}_0] = \beta\ln\frac{1-\alpha}{\beta} + (1-\beta) \ln \frac{\alpha}{1-\beta}. \tag{19}$$

Next, according to (14), the expectation of λ_t under $\mathcal{H}_k$ can be expressed as:

$$\mathbb{E}[\lambda_t|\mathcal{H}_k] = \frac{(\mu_1-\mu_0)\mathbb{E}\left[\sum_{i_t=1}^{n_t} r_{i_t}^k\right] + \frac{1}{2}\mathbb{E}\left[n_t({\mu_0}^2 - {\mu_1}^2)\right]}{{\sigma_0}^2}, \tag{20}$$

where $r_{i_t}^k$ is RSRP from the FAP we are detecting under hypothesis $\mathcal{H}_k$.

According to (18)–(20), we derive the average detection rounds in normal cases.

To further analyze the impacts of cooperation range, FAP transmission power, and user density, we need to derive the expectation of the sum of test statistics $\mathbb{E}[\sum_{i_t=1}^{n_t} r_{i_t}^k]$, which, however, has no closed-form expression. Thus, we approximate the test statistics as follows.

We first approximate $\mathbb{E}[\sum_{i_t=1}^{n_t} r_{i_t}^1]$. Note that test statistics follow the Gaussian distribution as described in (2). The expected sum of test statistics under $\mathcal{H}_1$ can be written as:

$$\mathbb{E}\left[\sum_{i_t=1}^{n_t} r_{i_t}^1\right] = \mathbb{E}\left[\sum_{i_t=1}^{n_t} r_{i_t}\mathcal{N}\left(P_{i_t} + N_o, {\sigma_0}^2\right)\right], \tag{21}$$

where P_{i_t} is the received signal strength from the FAP we are detecting. In practice, the measurement error (i.e., ${\sigma_0}^2$) is much smaller than RSRP. Thus, we can approximate (21) as follows:

$$\begin{aligned}\mathbb{E}\left[\sum_{i_t=1}^{n_t} r_{i_t}^1\right] &\approx \mathbb{E}\left[\sum_{i_t=1}^{n_t} P_{i_t}\right] + \mathbb{E}\left[\sum_{i_t=1}^{n_t} N_o\right] \\ &= P_o\mathbb{E}\left[\sum_{i_t=1}^{n_t}\left(\frac{d_o}{d_{i_t}}\right)^a\right]\mathbb{E}[e^X]\mathbb{E}[e^Y] + N_o\mathbb{E}[n_t],\end{aligned} \tag{22}$$

where P_o is FAP's transmission power in normal cases, $(\frac{d_o}{d_{i_t}})^a$ the user i's channel gain from path loss at time t, e^X and e^Y the shadow fading factor and multi-path fading factor, respectively. According to [21], the sum of interference of transmitters with a Poisson distribution to a receiver can be approximated as a log-normal distribution. Correspondingly, we can approximate the sum of the received FAP signal strengths at users with Poisson distribution as a log-normal distribution in a similar way. Thus, we have: $\mathbb{E}[\sum_{i_t=1}^{n_t}(\frac{d_o}{d_{i_t}})^a] \sim Log - \mathcal{N}(\mu_m, \sigma_m^2)$, where μ_m and σ_m^2 are given by [21]:

$$\mu_m = \frac{1}{2}\ln\left(\frac{m_1^4}{m_1^2+m_2}\right) \text{ and } \sigma_m^2 = \ln\left(\frac{m_1^2+m_2}{m_1^2}\right), \tag{23}$$

where m_k $(k=1,2)$ is the kth cumulant of $\sum_{i_t=1}^{n_t}(\frac{d_o}{d_{i_t}})^a$ given as: $m_k = \frac{2\rho\pi d_o^{ka}}{ka-2}(\frac{1}{\epsilon^{ka-2}} - \frac{1}{R^{ka-2}})$, where ρ is the user density, ϵ the minimum separation between a user and an FAP, and R the cooperation range. Only users within R will report their RSRP statistics to the MBS. In femtocell networks, we have $ka-2>0$ and $\epsilon \ll R$. Thus, m_k can be approximated as $m_k \approx \frac{2\rho\pi d_o^{ka}}{(ka-2)\epsilon^{ka-2}}$.

By far, we have derived all the expectations that are needed to compute the sum of test statistics, i.e., $\mathbb{E}[\sum_{i_t=1}^{n_t}(\frac{d_o}{d_{i_t}})^a] = e^{\mu_m + \frac{1}{2}\sigma_m}$, $\mathbb{E}[e^X] = e^{\frac{1}{2}\sigma}$ and $\mathbb{E}[e^Y] = 1$. For the average number of test statistics within cooperation range n_t, since user follow Poisson distribution, we have $\mathbb{E}[n_t] = \rho\pi R^2$.

Based on all the above analysis, we finally have $\mathbb{E}[\lambda|\mathcal{H}_1]$ to be approximated as:

$$\mathbb{E}[\lambda|\mathcal{H}_1] \approx \frac{(\mu_1-\mu_0)\rho\pi}{\sigma_o^2}\left(\left(N_o - \frac{\mu_1+\mu_0}{2}\right)R^2 + \frac{2P_o d_o^a e^{\frac{1}{2}\sigma^2}}{(a-2)\epsilon^{a-2}}\right).$$

Then, we derive $\mathbb{E}[\lambda|\mathcal{H}_0]$ as follows. According to (2), $\mathbb{E}[\sum_{i_t=1}^{n_t} r_{i_t}^1]$ can be expressed as:

$$\mathbb{E}\left[\sum_{i_t=1}^{n_t} r_{i_t}^0\right] = \mathbb{E}\left[\sum_{i_t=1}^{n_t} r_{i_t}\mathcal{N}(N_o, {\sigma_0}^2)\right] = N_o\rho\pi R^2. \tag{24}$$

Finally, the expected detection delay under $\mathcal{H}_1$ and $\mathcal{H}_0$ can be derived.

$$\mathbb{E}[T|\mathcal{H}_1] = \frac{{\sigma_0}^2(1-\alpha)\ln\frac{1-\alpha}{\beta} + {\sigma_0}^2\alpha\ln\frac{\alpha}{1-\beta}}{(\mu_1-\mu_0)\rho\pi\left(\left(N_o - \frac{\mu_1+\mu_0}{2}\right)R^2 + \frac{2P_o d_o^a e^{\frac{1}{2}\sigma^2}}{(a-2)\epsilon^{a-2}}\right)}, \tag{25}$$

$$\mathbb{E}[T|\mathcal{H}_0] = \frac{{\sigma_0}^2\beta\ln\frac{1-\alpha}{\beta} + {\sigma_0}^2(1-\beta)\ln\frac{\alpha}{1-\beta}}{\left(N_o - \frac{\mu_1+\mu_0}{2}\right)(\mu_1-\mu_0)\rho\pi R^2}. \tag{26}$$

Since α and β are predefined, we have the following observation based on (26):

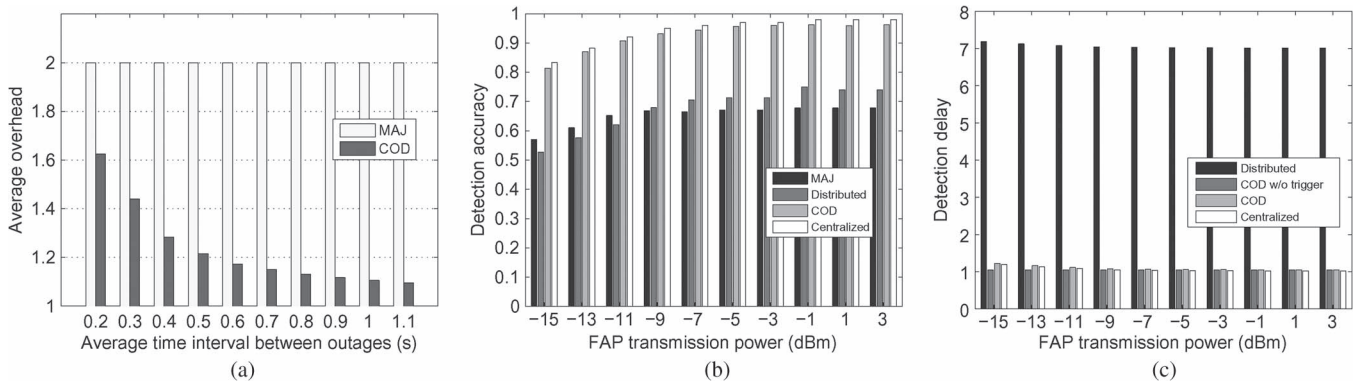

Fig. 3. Overall performance. (a) Average overhead. (b) Detection accuracy. (c) Detection delay.

Proposition 1: The average outage detection delay is inversely proportional to the user density and the cooperation area (i.e. πR^2), but is independent of the FAP's transmission power.

VII. Numerical Results

A. Simulation Setup

We consider a two-tier cellular network comprised of multiple femtocells overlaid on a macrocell. Femtocells are distributed randomly within an area of 1000 m $\times$ 1000 m. All FAPs operate at the carrier frequency of 2.5 GHz with 5 MHz channel bandwidth. Femtocell users are distributed randomly within the same area, and are associated with the FAP with the strongest RSRP. Users send their RSRP reports every 0.1 s. Each femtocell user moves according to the random waypoint mobility model [22] within the range of the network area. Each user moves with speed interval of [0,10] m/s, pause time interval of [0,1] s, and walk interval of [2, 6] s. The propagation model is determined based on the ITU and COST231 model which are described in [23] and [24]. The transmission powers of FAPs are set according to a self-configuring power control scheme [25]. The misdetection rate and false alarm rate parameters $\alpha = \beta = 0.01$. Unless explicitly otherwise stated, the numbers of FAPs and users are 100 and 1000, respectively, cooperation range $R = 600$ m, and the standard deviation of the shadow fading dB-spread $\sigma_{dB} = 8$ dB, where $\sigma_{dB} = 10\sigma/\ln(10)$. The simulation results are the average results from 5000 randomly generated network topologies.

To demonstrate the merits of the proposed statistic correlation based architecture, we compare COD with the commonly used maximum likelihood ratio based approach [26] referred to as MAJ. In MAJ, each user associated with the femtocell in normal state collects RSRP statistics, decides a binary hypothesis problem based on the maximum likelihood ratio, and reports the binary decision directly to the MBS. Then, the MBS makes the decision by majority vote. For a fair comparison, we enhance MAJ by collecting test statistics of the same number of detection rounds as with COD. Thus, both schemes have the same detection delay. To show the performance gain from spatial correlations, we also compare COD with distributed and centralized schemes, both of which adopt the same detection techniques as used in COD but exploits different spatial diversities: the distributed scheme detects outages based on RSRPs collected within each femtocells, while then centralized scheme detects outages by collecting all RSRPs within a macrocell.

B. Overall Performance

Fig. 3(a)–(c) illustrate the overall performance of COD, i.e., average overhead, detection accuracy and detection delay. Average overhead is defined to be the overall number of statistic reports transmitted in each detection round divided by the number of users. Detection accuracy is defined to be the probability of correctly detecting an outaged femtocell. Note that we do not show the false alarm rate in the figures since it is less than 0.001 in all cases, which is much higher than the misdetection rate. Detection delay is defined as the number of detection rounds. In Fig. 3(b) and (c), we set uniform transmission power for FAPs to evaluate the performance of COD under different transmission power levels. Fig. 3(a) shows that the average overhead of COD is smaller than MAJ when varying the average time interval between outages. The merit of COD comes from the distributed trigger mechanism. Note that in practice, the frequency of outages can be much lower (i.e., larger time interval), in which case the merits of COD are more obvious.

Fig. 3(b) depicts the detection accuracy for various FAP power levels, and it is shown that COD outperforms MAJ in detection accuracy by more than 20% in all cases demonstrated. We also see that the proposed scheme achieves similar accuracy compared to the centralized scheme, and outperforms the distributed scheme over 20% in all cases. This is because COD exploits spatial correlations by collaborative filtering and data fusion to obtain more information for the final decision, while MAJ simply aggregates statistics by majority vote.

From Fig. 3(c), we see that COD enjoys similar detection delay compared with the centralized scheme, and can detect outage within two detection rounds in all cases in the figure. Fig. 3(c) also indicates that the difference in the detection delays of COD without trigger stage and COD approaches zero when FAP transmission power increases. The reason is that as the FAP power gets larger, it is easier to differentiate outage cases from normal cases, the probability of immediately triggering the detection stage is higher. We also observe that the detection delay of COD without trigger stage is independent of the FAP transmission power, which matches our analytical results in Proposition 1.

VIII. Conclusion

This paper proposes COD, a cooperative detection architecture to detect femtocell outages. COD considers the challenges caused by the distinct features of the two-tier femto-macro networks, including dense deployments, vertical handover, and sparse user statistics. To resolve these issues, COD leverages collaborative filtering and sequential hypothesis detection to exploit the spatial and temporal correlations among RSRP statistics across different femtocells. Our evaluations show that our cooperative detection largely reduces communication overhead and achieves higher detection accuracy than the existing approach under the same delay condition. Both analytical and numerical results validate the correlation-based cooperative detection architecture, which can be used as a general framework for future femtocell outage detection scheme design. This paper also provides some guidelines through theoretical analyses and numerical evaluations.

References

[1] Telecommunication management; self-organizing networks (SON); self-healing concepts and requirements, 3rd Generation Partnership Project, Sophia-Antipolis Cedex, France, 3GPP TS 32.541, Mar. 2011, Rel. 10.

[2] "Self-organizing networks, NEC's propoals for next-generalization radio network management," NEC White Paper, 2009.

[3] C. Mueller, M. Kaschub, C. Blankenhorn, and S. Wanke, "A cell outage detection algorithm using neighbor cell list reports," in *Proc. Int. Workshop Self-Organizing Syst.*, 2008, pp. 218–229.

[4] R. Khanafer *et al.*, "Automated diagnosis for UMTS networks using bayesian network approach," *IEEE Trans. Veh. Technol.*, vol. 57, no. 4, pp. 2451–2461, Jul. 2008.

[5] 3G home nodeB (HNB) study item, 3rd Generation Partnership Project, Sophia-Antipolis Cedex, France, 3GPP TR 25.820, Mar. 2008.

[6] R. Chandra, V. N. Padmanabhan, and M. Zhang, "Wifiprofiler: Cooperative diagnosis in wireless LANs," in *Proc. ACM MobiSys*, 2006, pp. 205–219.

[7] A. Adya, P. Bahl, R. Chandra, and L. Qiu, "Architecture and techniques for diagnosing faults in ieee 802.11 infrastructure networks," in *Proc. ACM MobiCom*, 2004.

[8] O. G. Aliu, A. Imran, M. A. Imran, and B. Evans, "A survey of self organisation in future cellular networks," *IEEE Commun. Surveys Tuts.*, vol. 15, no. 1, pp. 336–361, 2013.

[9] W. Wang and Q. Zhang, "Local cooperation architecture for self-healing femtocell networks," *IEEE Wireless Commun.*, vol. 21, no. 2, pp. 42–49, Apr. 2014.

[10] "Evolved universal terrestrial radio access network (e-utran); self-configuring and self-optimizing network use cases and solutions," 3rd Generation Partnership Project, Sophia-Antipolis Cedex, France, 3GPP TR 36.902, Feb. 2012, Rel. 11.

[11] "Universal terrestrial radio access (utra) and evolved universal terrestrial radio access (e-utra); radio measurement collection for minimization of drive tests (mdt); overall description; stage 2," 3rd Generation Partnership Project, Sophia-Antipolis Cedex, France, 3GPP TS 37.320, Jun. 2011, Rel. 11.

[12] W. Wang, J. Zhang, and Q. Zhang, "Transfer learning based diagnosis for configuration troubleshooting in self-organizing femtocell networks," in *Proc. IEEE GLOBECOM*, Dec. 2011, pp. 1–5.

[13] V. Erceg *et al.*, "An empirically based path loss model for wireless channels in suburban environments," *IEEE J. Sel. Areas Commun.*, vol. 17, no. 7, pp. 1205–1211, Jul. 1999.

[14] S. Shellhammer *et al.*, "Performance of power detector sensors of DTV signals in IEEE 802.22 WRANs," in *Proc. ACM TAPAS*, 2006, p. 4.

[15] X. Chen, J. Huang, and H. Li, "Adaptive channel recommendation for dynamic spectrum access," in *Proc. IEEE DySPAN*, May 2011, pp. 116–124.

[16] J. Wang and D. Katabi, "Dude, where's my card? rfid positioning that works with multipath and non-line of sight," in *Proc. ACM SIGCOMM*, Aug. 2013, pp. 51–62.

[17] D. Cai, X. He, X. Wu, and J. Han, "Non-negative matrix factorization on manifold," in *Proc. IEEE ICDM*, Dec. 2008, pp. 63–72.

[18] N. Srebro, N. Alon, and T. Jaakkola, "Generalization error bounds for collaborative prediction with low-rank matrices," in *Proc. NIPS*, Dec. 2004, pp. 1–8.

[19] J.-H. Yun and K. G. Shin, "Ctrl: A self-organizing femtocell management architecture for co-channel deployment," in *Proc. ACM MobiCom*, Sep. 2010, pp. 61–72.

[20] A. Wald, "Sequential tests of statistical hypotheses," *Ann. Math. Statist.*, vol. 16, no. 2, pp. 117–186, Jun. 1945.

[21] R. Menon, R. Buehrer, and J. Reed, "On the impact of dynamic spectrum sharing techniques on legacy radio systems," *IEEE Trans. Wireless Commun.*, vol. 7, no. 11, pp. 4198–4207, Nov. 2008.

[22] C. Bettstetter, G. Resta, and P. Santi, "The node distribution of the random waypoint mobility model for wireless Ad Hoc networks," *IEEE Trans. Mobile Comput.*, vol. 2, no. 3, pp. 257–269, Jul.–Sep. 2003.

[23] "Guidelines for evaluation of radio transmission technologies for imt-2000," Int. Telecommun. Union, Geneva, Switzerland, ITU-R Rec M.1225, 1997.

[24] "Digital mobile radio towards future generation systems: Final report," Eur. Commission, Brussels, Belgium, COST Action 231, 1999.

[25] D. López-Pérez, X. Chu, A. V. Vasilakos, and H. Claussen, "On distributed and coordinated resource allocation for interference mitigation in self-organizing lte networks," *IEEE/ACM Trans. Netw.*, vol. 21, no. 4, pp. 1145–1158, Aug. 2013.

[26] H. Akaike, "Information theory and an extension of the maximum likelihood principle," in *Proc. IEEE ISIT*, Jul. 1973, pp. 267–281.

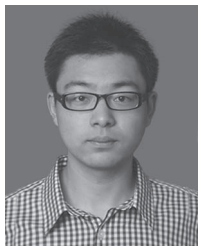

Wei Wang (S'10) received the B.E. degree in electronics and information engineering from Huazhong University of Science and Technology, Wuhan, China, in 2010. He is pursuing the Ph.D. degree in Hong Kong University of Science and Technology. His research interests include privacy, fault management and PHY/MAC design in wireless networks.

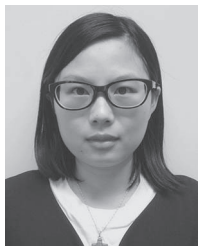

Qing Liao (S'10) received B.Sc. degree in software technology and application from Macau University of Science and Technology, Macau, in 2010 and the M.Phil. degree in computer science and technology from the Fok Ying Tung Graduate School of Hong Kong University of Science and Technology in 2013. She is currently pursuing the Ph.D. degree in Hong Kong University of Science and Technology. Her research interests include wireless networks and machine learning.

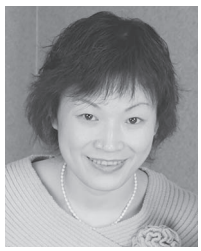

Qian Zhang (M'00–SM'04–F'12) received the B.S., M.S., and Ph.D. degrees from Wuhan University, China, in 1994, 1996, and 1999, respectively, all in computer science. She joined Hong Kong University of Science and Technology in Sept. 2005 where she is now a full Professor in the Department of Computer Science and Engineering. Before that, she was in Microsoft Research Asia, Beijing, from July 1999, where she was the Research Manager of the Wireless and Networking Group. She has published 300 refereed papers in international leading journals and key conferences in the areas of wireless/Internet multimedia networking, wireless communications and networking, wireless sensor networks, and overlay networking. She is a Fellow of IEEE for "contribution to the mobility and spectrum management of wireless networks and mobile communications". Dr. Zhang has received MIT TR100 (MIT Technology Review) worlds top young innovator awards. She also received the Best Asia Pacific (AP) Young Researcher Award elected by IEEE Communication Society in year 2004. Her current research is on cognitive and cooperative networks, dynamic spectrum access and management, as well as wireless sensor networks.